



Synthesis and application of various metal oxide–/biomaterial–coated carbonaceous nanomaterials derived from waste biomass for removal of Cr⁺⁶ present in solution

Vijoyeta Chakraborty¹ · Papita Das^{2,3} · Pankaj K. Roy¹

Received: 17 October 2020 / Revised: 7 December 2020 / Accepted: 15 December 2020 / Published online: 3 January 2021
© The Author(s), under exclusive licence to Springer-Verlag GmbH, DE part of Springer Nature 2021

Abstract

In this study, seven different nanocoated carbonaceous materials was synthesized using hydrothermal method. Graphene oxide and activated carbon from biochar of sawdust were used as matrix materials, and the coating materials used were mainly nanoparticles, lanthanum oxide, cerium oxide, zirconium oxide, and cellulose. The adsorption capacities of these composites were analyzed by estimating the removal capacity for the hexavalent chromium present in the solution. Parameters like adsorbent dose, pH, and metal ion concentration were studied. The composites prepared by coating activated carbon with functionalized graphene oxide and zirconium oxide had shown higher removal capacity more than 160 mg/g in acidic pH, i.e., pH 4 with 1 mg/ml adsorbent dose and up to 150 mg/l of hexavalent chromium concentration. The removal capacity was second for the activated carbon coated with graphene oxide and third highest value obtained from the composite prepared by coating activated carbon synthesized from biochar with zirconium oxide. The removal capacity obtained was directly related to the surface area and the presence of active surface functional group. The study aims to provide a better nanocoated composite for removal of hexavalent chromium present in the experimental solution.

Keywords Nanocomposite · Synthesis · Characterization · Hexavalent chromium · Adsorption

1 Introduction

The nanocomposites are included into the field of material science which deals with everyday life usage like automobile industries, making of sensors, energy devices, and also in pollution abatement tools [32]. Nanocomposites were generally made up to two or more material, with at least one of them having structure in nanoscale, i.e., between 1 and 100 nm [14]. The nanostructure gives the composite more stability and enhanced functional activity. The matrixes of the composites are mainly polymers, metals, biomass, or ceramic. They have

their own demerits, like their functional activity was low before the incorporation of nanomaterials into the polymer matrix. The applicability of the nanocomposite in water purification system was studied thoroughly by many research workers. The need for freshwater is one of the common resources which the living organisms are craving for. The industrial discharge had made the freshwater sources polluted. The use of nanocomposite in treating the polluted water could provide a solution. The nanostructure made the composites more efficient in treating the polluted water. The high surface area of the composite could highly influence the water purification process.

The nanocomposites were made up of matrix material and filler material. The filler was mostly in nanoscale, and the matrix material could be both organic and inorganic material. Mostly used organic materials in composite preparation are biomass or some biomaterial like sawdust, sugarcane bagasse, and rice husk. The inorganic materials used in composite preparation were synthetic polymers, metal oxides, etc [1, 2]. The used matrix material in composite formation made different groups of composite. If the matrix material used were metal, the composite was known as metal matrix composite; if

✉ Papita Das
papita.das@jadavpuruniversity.in

¹ School of Water Resources Engineering, Jadavpur University, Kolkata, India

² Department of Chemical Engineering, Jadavpur University, Kolkata, India

³ School of Advanced Studies in Industrial Pollution Control Engineering, Jadavpur University, Kolkata, India

the matrix used were polymer, then it was named as polymer matrix composite; and if some biomass was used as a matrix material, then it was known as biopolymer matrix composite.

The preparation of nanocomposites have many routes; they can be prepared by solution blending [47], melt processing [10], in situ polymerization [46], and sol-gel method [11]. The preparations of biopolymer composites have many good environmental effects, due to its permeability in water, biocompatibility, and biodegradable nature [9]; the usage of this biomaterial for many processes in pollution abatement provides an economical, sustainable, and environment-friendly solutions. There are many existing methods for making biocomposites like hydrothermal synthesis, co-precipitation method (Zhang *et al.*, 2006, Cho *et al.*, 2006 and Godinho *et al.*, 2007), and solution dispersion method [15, 27, 39]. The coating of matrix with nanomaterials enhances their thermal stability, which helped in treating the wastes which need more temperature to degrade. Some adsorption processes need higher temperature for proper functioning of the adsorbent, so the thermally stable adsorbent could be used for in wide temperature variations. The composites prepared by biomaterial had some bonus advantages, since the biomass used for making the nanocomposite has many surface active functional groups, which not only provide more binding sites for pollutant entrapment but also give more roughness and stability to the composite [21, 22].

In this study synthesis of different metal/bionanocomposites were studied. The composites used in this study were mainly metal matrix composites, biocomposites and incorporation of both metal and biocomposites on carbonaceous materials. The enhanced functionality of the synthesized nanomaterial was analyzed and the application of these nanocomposites for removal of a very toxic and hazardous but widely used heavy metals were studied, i.e., hexavalent chromium (Cr^{+6}).

The use of agricultural waste (sawdust) as matrix material for the making of bionanocomposites would provide an environment friendly solution for nanocomposite preparation and waste minimization. The use of graphene oxide as matrix material would give an enhanced functional stability and surface area for preparation of metal matrix composites.

Graphene oxide had many positive applications in water treatment technology. The surface area and presence of active surface functional group and its honeycomb-like porous structure and highly biocompatible play an important role in pollutant entrapment in its surface [7]. The presence of sp^2 hybridized carbon made it more competent as composite.

This study deals with preparation of different composites and reviewing its applicability in hexavalent chromium removal. The use this of heavy metal is wide in many industries like electro plating, lather tanning, dye, and pigment industries. The discharge of Cr^{+6} from these industries made the pathway for bioaccumulation of these metals to life in different tropic levels. The exposure of Cr^{+6} to living body causes

stomach irritation, skin cancer, and ulceration [36]. Chrome hole is a potent form of skin cancer commonly found in workers working in lather tanning industries [3]. The treatment of this toxic waste was very much in need for recent time.

The use of nanocomposites in treatment of pollutants would provide an extensive scope for research work in this filed, due to its high functionality in water treatment technology [20]. The use of biomass as the matrix material could provide an additional benefit as they contain a highly porous structure and many active surface functional groups into its surface. The composites used in this study were made up with two different matrix materials: graphene oxide and activated carbon from biochar of sawdust. The filling material used was mainly nanoparticles, lanthanum oxide, cerium oxide, zirconium oxide, cellulose, etc. Coating on activated carbon by synthesized surface functionalized graphene oxide was also studied. The removal capacity of Cr^{+6} by the synthesized nanocoated carbonaceous materials was evaluated, and the parametric effect of the removal was studied. The removal of Cr^{+6} using nanocomposite was studied by many researchers like Shang *et al.* [37], Su *et al.* [40], and Chakraborty *et al.* [5]. The use of nanocomposite in treating this hazardous pollutant was thoroughly studied in this study, a comparative study was done in the present research work, and some new composites were prepared which were not properly studied by previous researcher.

2 Materials and methodology

2.1 Materials

Raw sawdust, sodium hydroxide (NaOH), potassium permanganate (KMnO_4), sulfuric acid (H_2SO_4), phosphoric acid (H_3PO_4), hydrogen peroxide (H_2O_2), hydrochloric acid (HCl), sodium hypochlorite (NaOCl), graphene oxide (GO), cerium oxide (CeO), zirconium oxide (ZrO), lanthanum oxide (LaO), carbinol, aqueous ammonia, acetone, lanthanum nitrate, hydrazine hydrate, zirconium oxychloride, potassium dichromate ($\text{K}_2\text{Cr}_2\text{O}_7$), and di-phenyl carbazide (DPC). All the chemicals used were lab grade and purchased from Merck and Platonic India Pvt. Ltd.

2.2 Coated composite preparation

Different types of composites were prepared using sawdust as the base materials for composites. Different forms of nanocomposites were prepared using activated carbon of sawdust with the metal oxides as coating materials to increase the adsorption and surface activity of the composite.

2.2.1 Thermally activated sawdust

The raw sawdust was washed with distilled water for removing dust and dirt and then treated with 0.1 N NaOH. The sawdust were again washed with distilled water to neutralize the base and washed repeatedly till it comes to neutral pH. Then, the sawdust was oven dried overnight and sealed in an air tight container. Five grams of that treated sawdust was pyrolyzed to prepare biochar at 700 °C and activated and then sieved with 300 µm sieve. The activated carbon was further used for making other nanocomposites [4].

2.2.2 Graphene oxide

Graphene oxide was prepared from graphite powder by using modified Hummers method [23]. In 20 g potassium permanganate (KMnO₄), 90 ml conc. H₂SO₄ and 60 ml H₃PO₄ were added gently. After 30 min of continuous, stirring 30 ml of H₂O₂ was added. The solution turned to yellowish brown. The whole solution was then sonicated for 120 min at 30 °C and washed repeatedly by 2% HCl until the solution comes to neutral pH (Elrouby et al., 2018). The graphene oxide obtained was then kept at a vacuum drier at 70 °C till it dried completely and stored at an air tight container. This synthesized graphene oxide was used for further composite preparation.

2.2.3 Cellulose extraction from sawdust

In distilled water, 30 g clean and oven dried sawdust was mixed and heated till 90 °C for 30 min for removal of any excess dirt and dust from the sawdust surface and to remove the impurities and chemicals used while wood processing. After heating, the sawdust was filtered out of the solution and treated with 300 ml of 1 M HCl solution for another 30 min at 85 °C. After this acid treatment, the solution was again washed two times using 0.5 M HCl. Then, alkali treatment was initiated. For this treatment, 10% NaOH solution was poured into the acid treated sawdust and the solution was heated for 90 min at 150 °C. This step was done to remove lignin from the raw material. The color of the sawdust now became light yellowish; now, the pulpy sawdust extract was treated with bleaching agent. This step was known as bleaching step; this is the final step for extraction of cellulose. In this step, the insoluble residue of the sawdust extract was filtered and washed repeatedly with distilled water. To remove the remaining part of lignin from the extract, 1% NaOCl or sodium hypochlorite was added to the pulp and heated till 95 °C for 60 min. This step was done thrice to remove all the lignin. Now, a white pulp of cellulose was left, which was washed repeatedly with distilled water and made it pH 7 [24]. Finally, the obtained cellulose was dried for 24 h at 50 °C in a vacuum drier to obtain the powdered form of

cellulose. The dried cellulose was pre iced at –20 °C and lyophilized at –45 °C for 4 h. The powdered cellulose was then stored in an air tight container.

2.2.4 Activated carbon coated with graphene oxide

The nanocomposite was prepared by solvo-thermal process. The nanocomposite was made with 10 g of activated carbon with 300 mg graphene oxide. At first, the activated carbon was mixed thoroughly in 100 ml distilled water in stirrer for 2 h, and 300 mg graphene oxide was mixed with 50 ml carbinol and sonicated for 1 h. Then, both solutions were mixed in a conical and sonicated for another half an hour. The resultant solution was poured in the Teflon flux and refluxed for 12 h at 120 °C. Then, the solution was allowed to settle and the supernatant was decanted and the filtrate was washed with ethanol and dried in a vacuum oven for 12 h at 80 °C. The composite was stored in an air tight container.

2.2.5 Graphene oxide coated with cerium oxide, lanthanum oxide, and zirconium oxide

Aqueous ammonia was used to dissolve cerium oxide (CeO), and pH was maintained at 11. The whole solution stirred for 3 h. On the other hand, 0.5 mg/ml of GO was sonicated for 3 h separately at acetone media. The CeO solution and the GO were then mixed slowly and stirred for another 3 h at a magnetic stirrer. The mixture was then poured at the Teflon flask and autoclaved for 14 h at 120 °C by a solvo-thermal process. After the autoclaving, the sample solution was kept for specific period of time. The mixture was taken out of the reactor and cooled, then mixture repeatedly washed with water ethanol mixture and centrifuged, and the supernatant was decanted. The nanocomposite obtained was then vacuum dried at 80 °C for 5 h to obtain the powdered nanocomposite.

For preparation of GO coated with lanthanum oxide composite, 100 ml of acetone was used as a dispersing media for GO dispersion. GO 0.5 mg/ml solution was used for making this composite; the solution was sonicated for 2 h. Twenty milliliters of aqueous solution of lanthanum nitrate was sonicated separately for 2 h. Thirty milliliters of hydrazine hydrate was then mixed to form the lanthanum oxide solution. Both the sonicated GO solution and LaO solution were mixed together and stirrer for 2 h. The mixture was then poured at the Teflon-coated hydrothermal autoclave reactor for 10 h at 150 °C by Zhang et al. [45, 37]. The mixture was taken out of the reactor and cooled, then mixture repeatedly washed with water and centrifuged, and the supernatant was decanted. The nanocomposite obtained was then vacuum dried at 100 °C for 24 h to obtain the powdered nanocomposite.

The third composite made up of zirconium oxide (ZrO)–coated GO was prepared by using 0.5 mg/ml GO in 100 ml acetone solution, which was sonicated for 2 h. On the other

hand, 0.5 g zirconium oxychloride was dissolved in 30 ml aqueous solution. One milliliter of hydrazine hydrate was added to the solution and stirred in a magnetic stirrer for 2 h. After 2 h, both the sonicated GO solution and the ZrO solution were mixed in a beaker and stirred for 1 h. The mixture was then poured in a Teflon flask and refluxed for 12 h at 180 °C by using hydrothermal reactor. After the autoclaving, the sample solution was kept for specific period of time [30]. The mixture was taken out of the reactor and cooled, then mixture repeatedly washed with water and centrifuged, and the supernatant was decanted. The nanocomposite obtained was then vacuum dried at 100 °C for 12 h to obtain the powdered nanocomposite.

2.2.6 Cellulose coated with graphene oxide

The cellulose and graphene oxide were prepared in laboratory. GO (0.07 g) was dissolved in double distilled water and sonicated for 1 h at room temperature. Simultaneously, 0.7 g cellulose was dissolved in double distilled water and sonicated for 1 h. Then, both the solutions were mixed and 2.33 ml aqueous ammonia was added to the mixture and stirred for 1 h. The mixture was then poured in a Teflon flask and refluxed for 12 h at 100 °C by using hydrothermal reactor. After the autoclaving, the sample solution was kept for specific period of time. The mixture was taken out of the reactor and cooled, then mixture repeatedly washed with water and centrifuged, and the supernatant was decanted. The nanocomposite obtained was then freeze dried for 24 h to obtain the powdered nanocomposite [38].

2.2.7 Activated carbon coated with zirconium oxide

Activated carbon (AC) obtained from sawdust (as described earlier) was used here to make the composite. Eight of activated carbon was added to 30 ml of carbinol solution and stirred in a magnetic stirrer for 1 h and then sonicated for 2 h to make a homogeneous mixture. The coating was done with zirconium oxide nanoparticles (ZrO np). So to enhance the surface activity of the activated carbon, its surface coating was done. Five hundred milligrams of ZrO nanoparticle was added in 50 ml H₂O₂ solution. Along with the ZrO nanoparticle, 500 mg of NaOH was also added and the whole mixture was sonicated for 30 min. Then, both the activated carbon solution and ZrO solution were mixed and overnight at 35 °C for mixing properly and forming a strong bond between AC and ZrO np. Then, the mixture was then poured in a Teflon flask and refluxed for 8 h at 180 °C by using hydrothermal reactor. After the autoclaving, the sample solution was kept for specific period of time [29]. The mixture was taken out of the reactor and cooled, then mixture repeatedly washed with water and centrifuged, and the supernatant was decanted. The nanocomposite obtained was then vacuum

dried at 100 °C for 12 h to obtain the powdered nanocomposite.

2.2.8 Activated carbon coated with graphene oxide–zirconium oxide nanocomposite

Eight grams of AC was dispersed in 30 ml of 1:1 water ethanol bath and then sonicated for 1 h. The well-dispersed AC solution was then fitted in a magnetic stirrer, and slowly, 800 mg of graphene oxide–zirconium oxide nanocomposites was added to it. Then, 0.5 ml NaOH and 0.5 ml H₂O₂ solution were added to the mixture and stirred for another 2 h. Then, the mixture was then poured in a Teflon flask and refluxed for 8 h at 180 °C by using hydrothermal reactor. After the autoclaving the sample solution for specific period of time, the mixture was taken out of the reactor and cooled, then mixture repeatedly washed with water and centrifuged, and the supernatant was decanted. The pH of the sample was made neutral by repeated washing and then vacuum dried for 24 h at 80 °C. The powder obtained was stored in air tight container.

2.3 Characterization of the composites

All the synthesized composites were characterized by different characterization techniques. The structural morphology of the synthesized nanocomposites was studied using SEM (scanning electron microscope analysis), the presence of surface active functional groups was detected using FTIR analysis (Fourier transformation infrared spectroscopy), and the crystalline structure of the composites was analyzed using XRD analysis (X-ray diffraction). The thermal stability of the synthesized composites was studied using TGA analysis (thermo-gravimetric analysis). Lastly, one of the most important parameters for structural analysis was done, i.e., surface area analysis, using BET (Brunauer–Emmett–Teller) nitrogen adsorption analysis.

2.4 The adsorption efficiency study of the composites

The efficiency of the prepared composites was studied by removing one of the toxic pollutant present in nature, i.e., hexavalent chromium (Cr⁺⁶). All the nanocomposites were characterized to know its physical and chemical properties. The parameters optimized in this study were pH, adsorbent dose, and initial. The detailed study of pH from pH 2 to pH 10, adsorbent dose from 1 to 10 mg/ml, and contact time from 15 to 120 min were studied. The samples were collected and analyzed by di-phenyl carbazide (DPC) method [3].

2.4.1 Removal of chromium using the composite

All the composites were taken into 50 ml Cr⁺⁶ solutions. For pH this study, different pH 2, 4, 6, 8, and 10 were made with

50 mg/l Cr^{+6} solutions. Adsorbent dose was kept constant with 1 mg/ml, and the study was done for 120 min. For optimizing adsorbent dose, different adsorbent doses were studied: 1 mg/ml, 2 mg/ml, 5 mg/ml, and 10 mg/ml. The optimized pH was maintained throughout this study, and the study was done for 120 min. Lastly, the effect of different concentrations of metal were studied to know the capacity of the composite to remove high concentration of pollutants. All the experiments were performed in triplicate, and the data were plotted in the form of adsorption capacity in graphs. The capacity of the composite to remove Cr^{+6} was studied using the following equation [22]:

$$q_e = (C_0 - C_e) \frac{v}{m} \quad (1)$$

q_e capacity of adsorbent for metal removal (mg/g)
 C_0 initial metal ion concentration (mg/l)
 C_e final metal ion concentration (mg/l)
 v volume of metal solution used in this experiment (l)
 m amount of adsorbent used in this experiment (g)

2.4.2 Preparation of Cr^{+6} stock solutions:-

Potassium dichromate (141.4 mg) was dissolved in 1000 ml distilled water to make 50 mg/l stock solution. Standard solutions were prepared by diluting the stock solution.

3 Results and discussion

3.1 Characterization of composites

3.1.1 FTIR analysis

Activated carbon obtained from pyrolysis of sawdust was analyzed in FTIR (PerkinElmer Spectrum Version 10.4.4, Waltham, USA). A sharp peak at 1029/cm was obtained which denoted the presence of –OH group and C–O group of –COOH, the peak observed at 3335/cm indicated the presence of –OH group, the presence of another sharp peak at 2914/cm indicated the presence of C–H stretching, and 1596/cm and 1228/cm peaks indicated the presence of C=O groups [4, 16]. The presences of negatively charged functional groups in the composite could be responsible for the removal of many heavy metals. The presence of hydroxyl group was mainly obtained from lignocelluloses of the sawdust. These functional groups were mainly provided the active sorption sites for pollutant removal, which in turn help in adsorption process (Fig. 1a). The activated carbon obtained from biochar had less number of functional group present than graphene oxide–modified biochar [38]. Similar result was obtained

from sawdust based activated carbon and graphene oxide composite. A characteristic peak at 3426/cm was obtained that indicated the presence of hydroxyl group like C=O group. The peak obtained at 1722/cm and 1263/cm could be attributed to C–C and C–OH groups, respectively. The presences of C–O–C and aromatic compounds were validated by vibration stretching at 1002/cm and 766/cm. The presence of these functional groups indicated that the composite formation was successfully done (Fig. 1b). The graphene oxide coated with different metal oxides was also studied through FTIR spectra. The graphene oxide composites included coating the graphene material with cerium oxide, lanthanum oxide, and zirconium oxide. The cerium oxide composites had four sharp distinct peaks at 3745/cm, 2923/cm, 1568/cm, and 1186/cm. The peak at 3745/cm indicated the presence of –OH group. Anti-symmetric stretching of –CH₂ group was indicated by the peak obtained at 2923/cm. The –OH group and C=O group were indicated by the other two groups [42] (Fig. 1c). The composite was prepared from coating graphene oxide with lanthanum oxide; the peak obtained near 3500/cm indicated the –OH vibrational stretching. The peaks near 1500/cm and 1100/cm indicated the presence of –COOH group which usually is found in graphene oxide surface. The small peak observed near 500/cm indicated the presence of lanthanum oxide in the composite [18, 24, 27] (Fig. 1d). By analyzing the FTIR spectra of surface, functionalized GO with zirconium oxide had shown four distinct peaks at 2925/cm, 1120/cm, 748/cm, and 502/cm (Fig. 1e). The peak at 1120 indicated the presence of –OH group of Zr–OH compound [29]. Anti-symmetric stretching of –CH₂ group was indicated by the peak obtained at 2923/cm. The –OH group and C=O group were indicated by the other two groups [42]. Peak (502/cm) may be formed due to ZrO stretching at GO nanosheet. Peak at 1120/cm was present due to CH₂ anti-symmetrical stretching of ZrOZr, the nanocomposite [17]. The composite prepared from coating cellulose with graphene oxide had distinct peak at 3399/cm that indicated the presence of hydroxyl group like C=O group; peak at 2925/cm was described earlier. The peak at 1061/cm indicated the hydroxyl stretching of the composite. In total, 1744/cm, 1451/cm, and 622/cm were some of the other peaks that indicated the composite formation (Fig. 1f). The activated carbon was coated with zirconium oxide nanoparticles to improve its function in pollutant removal. The FTIR spectra showed some distinct peaks at 2926/cm, 1787/cm, and 1384/cm. The peaks obtained here were almost similar with the graphene oxide composite; the presence of C=O stretching was very prominent by analyzing these peaks (Fig. 1g). The peak at 1384/cm indicated –C–OH group [18]. The last composite which was prepared by coating the activated carbon with surface functionalized graphene oxide was analyzed, and the following peaks were obtained: 2926/cm was described earlier. The peak 1747/cm indicated the presence of C=O group; the peaks at 1557 and 1145

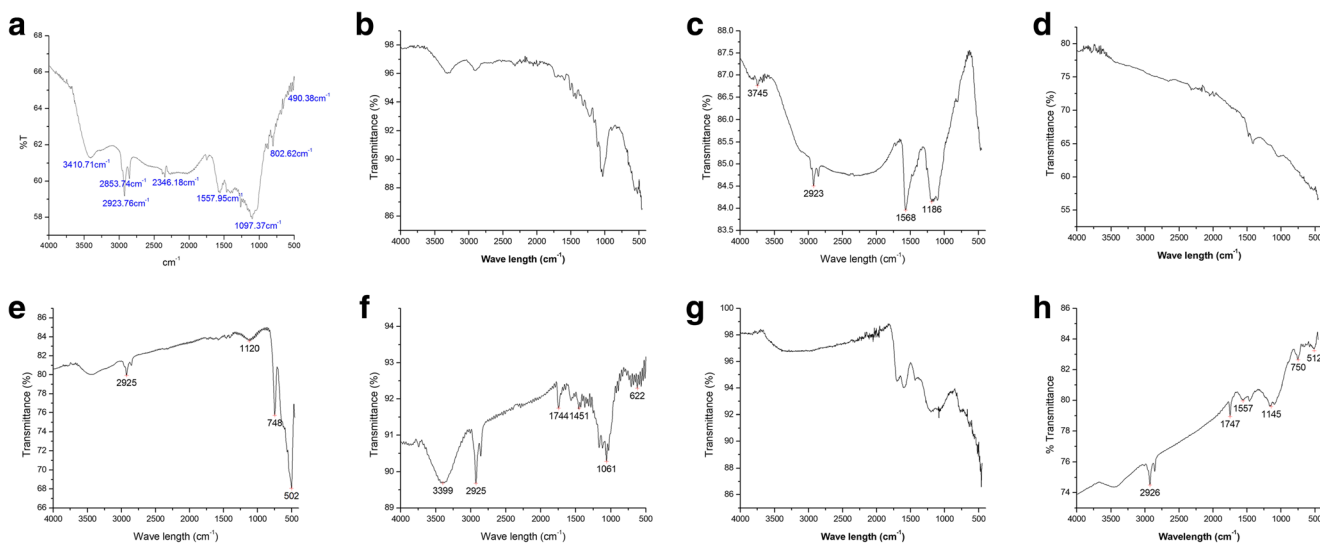


Fig. 1 Fourier transformation infrared spectroscopy (FTIR) analysis. **a** Thermally activated sawdust. **b** Activated carbon coated with graphene oxide. **c** Graphene oxide coated with cerium oxide. **d** Graphene oxide coated with lanthanum oxide. **e** Graphene oxide coated with zirconium

oxide. **f** Cellulose coated with graphene oxide. **g** Activated carbon coated with zirconium oxide. **h** Activated carbon coated with graphene oxide-zirconium oxide nanocomposite

indicated the –OH stretching. The peak at 750 indicated the bond formation of C–O–C group. The peak at 502/cm was formed due to the presence of the metal bonding with GO sheet (Fig. 1h).

3.1.2 SEM analysis

SEM (ZEISS EVO-MA 10, Carl Zeiss Microscopy, USA) images were analyzed to know the composites surface morphology. The porous structure of sawdust had a great potential for pollutant removal. The surface active functional group and the porous structure influence the removal capacity of the composites. To improve its adsorption capability, surface coating was done. The coating material includes cerium oxide, graphene oxide, zirconium oxide, and lanthanum oxide. The micro- and mesoporous structures of thermally modified sawdust or activated carbon were evident from Fig. 2a. Then, the sawdust was coated with graphene oxide to increase its surface activity. Since graphene oxides had high surface area and contain many oxygenated functional group, so a good composite was made out of it. Figure 2b shows the two-dimensional structure of graphene oxide which had many uniformly distributed pores, and Fig. 2c shows the composite prepared from coating activated carbon derived from sawdust with GO. The highly porous structure of thermally modified sawdust was enhanced with surface coating it with GO. The surface coating was clearly visible. The presence of graphene sheet on the embedded surface was visible in this figure. The surface activity of the thermally modified sawdust was increased by coating the surface of the biochar with zirconium oxide nanoparticles (Fig. 2d). The thermally modified sawdust coated with these nanomaterials enhances the surface activity

of the composite, hence increasing the removal efficiency of these composites for pollution abatement. The coating of biochar with surface functionalized graphene oxide coated with zirconium oxide nanoparticle is shown in Fig. 2e. The surface activity and surface area of these composite were highly increased with these surface modifications. The images shown in this section for composite preparation show uniform surface morphology.

3.1.3 XRD analysis

The thermally modified sawdust had shown three different peaks at 25.65°, at 29.45°, and at 43.27° indicating the presence of lignin and tannin causing the amorphous structure [33] shown in Fig. 3a. The presence of crystalline cellulose was also observed by studying the peak at 25.65° [36]. The characteristic peak of GO at 10° was obtained by XRD analysis (PANalytical X-PERT PRO, Malvern Panalytical, UK) of the sample prepared for making the composites as shown in Fig. 3b that was obtained from XRD analysis; a sharp peak was obtained at $2\theta = 11.9^\circ$ indicating the interlayer spacing of composite containing layered structure, and this peak may be due to the presence of GO into the nanocomposite. The XRD peaks at 20.66° and 25.24° are also typical for the presence of GO or by the reduced GO. The sharp peak at 26.38° indicated the crystallinity of cellulose in sawdust based activated carbon. The peak obtained at 49.86° indicated graphite-like structure, which can be formed due to carbonization of sawdust [5]. The composite was made up of cellulose and graphene oxide. Figure 3c shows distinct peaks at 22.8°, 16.34°, and 34.7°; these peaks were typically found when crystalline cellulose is present into the composite [6, 19, 24].

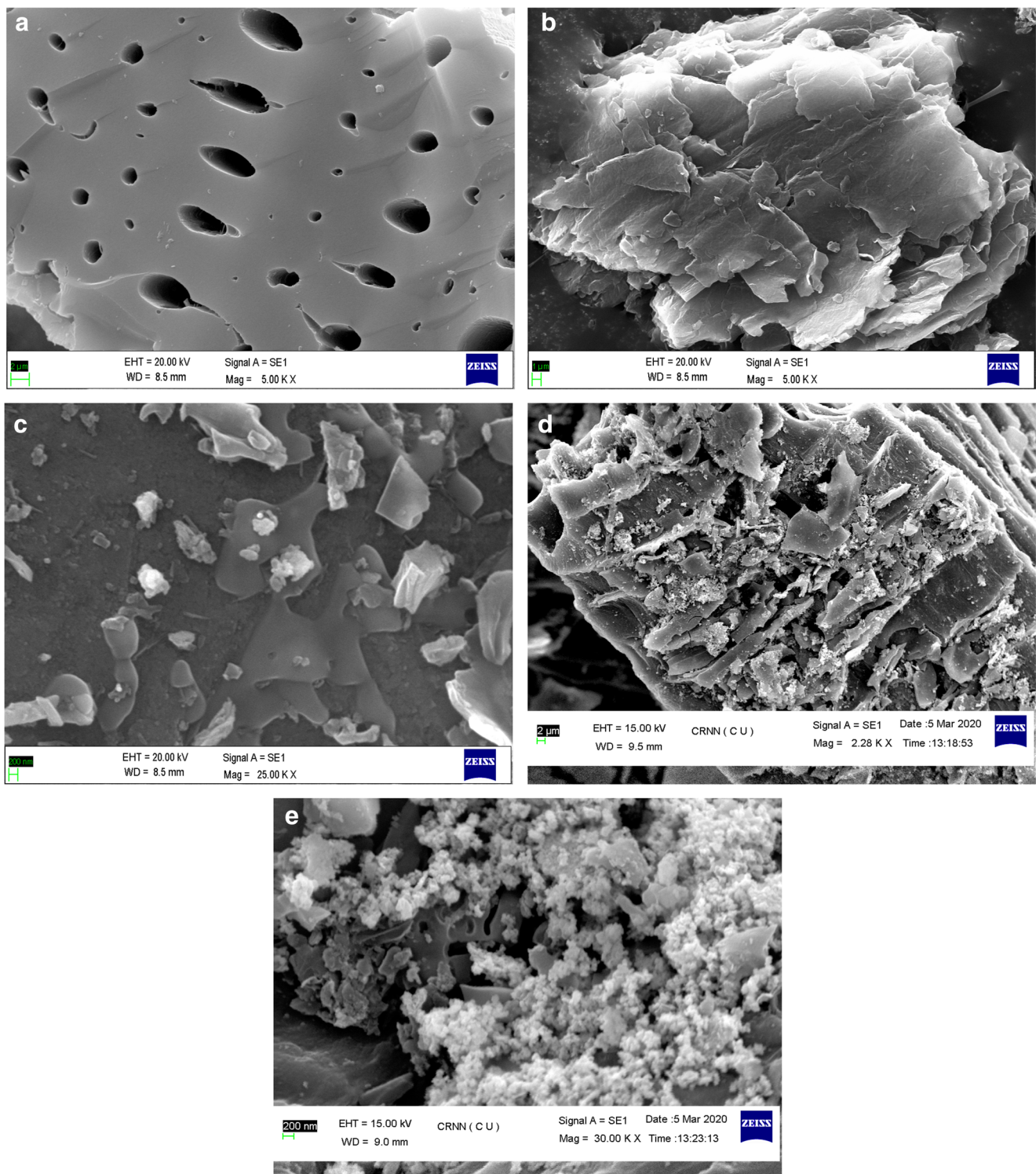


Fig. 2 Scanning electron microscope (SEM) analysis. **a** Thermally activated sawdust. **b** Graphene oxide. **c** Activated carbon coated with graphene oxide. **d** Activated carbon coated with zirconium oxide. **e** Activated carbon coated with graphene oxide–zirconium oxide nanocomposite

The composite made of graphene functionalized with zirconium oxide is shown in Fig. 3d showing some distinct peaks at 28.25° and 34.25° that were observed indicating short layers stacked in reduced graphene oxide [30]. Peaks at 40.85° ,

50.2° , and 60° show the composite formation. The surface coating of graphene oxide with lanthanum was analyzed by XRD peaks at 20.4° and 26.25° ; the presence of reduced GO was indicated by peak at 26.25° [35]. The peak obtained at

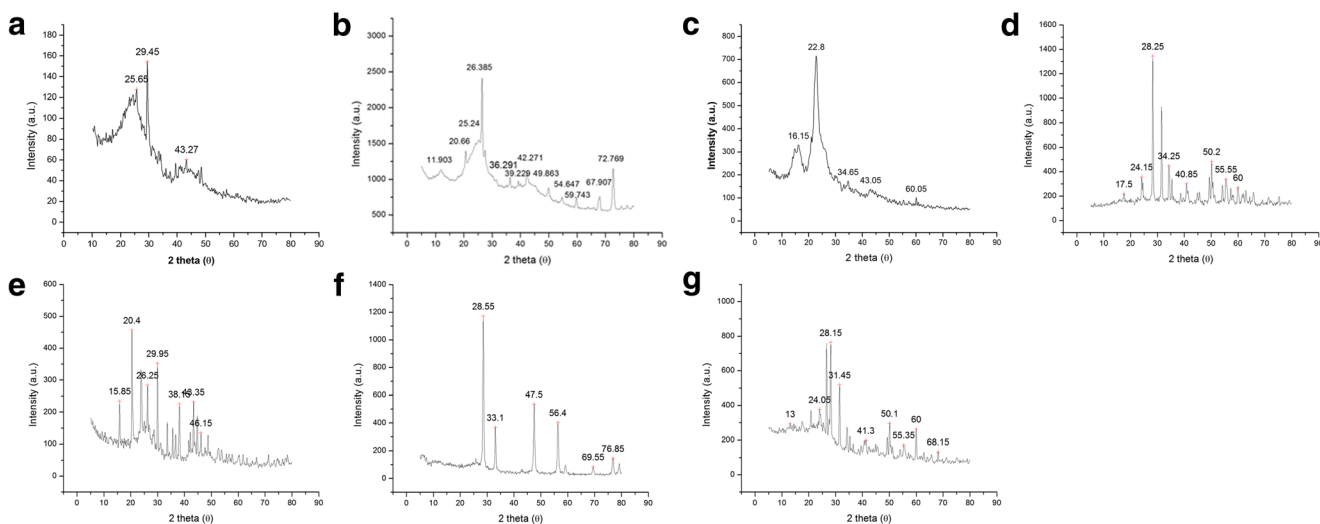


Fig. 3 X-ray diffraction (XRD) analysis. **a** Thermally activated sawdust. **b** Activated carbon coated with graphene oxide. **c** Cellulose coated with graphene oxide. **d** Graphene oxide coated with zirconium oxide. **e**

Graphene oxide coated with lanthanum oxide. **f** Graphene oxide coated with cerium oxide. **g** Activated carbon coated with graphene oxide–zirconium oxide nanocomposite

29.947° indicated the presence of La_2O_3 . The peak at 46.15° indicated the presence of LaC_2 . The rest of the distinct peak indicated the formation of Ancyrite (Fig. 3e). The composite prepared by coating GO with cerium oxide was studied using XRD shown in Fig. 3f. Peak at 28.55° indicated the presence of cerium oxide; the rest of the peak obtained by analyzing these composites also suggests the presence of cerium oxide. This result indicated uniform surface coating of the GO surface with cerium oxide. The final composite studied through XRD analysis was surface-coated activated carbon by surface functionalized GO with zirconium oxide. Since the composite was made up of different oxygenated compounds, different distinguished peaks were obtained by analyzing this composite. The peak obtained at 13° indicated the strong presence of GO. The peaks obtained at 24.05°, 28.15°, 41.3°, 50.1°, and 55.35° indicated the presence of zirconium oxide. The rest of the peaks indicated the formation of mestranol ($\text{C}_{21}\text{H}_{26}\text{O}_2$). Lignocellulosic compound was commonly found in majority of the pyrochars. The presence of these structures indicated a good composite formation (Fig. 3g).

3.1.4 TGA

The thermal stability of the prepared composites was estimated using this TGA analysis (STA 6000, PerkinElmer, USA) (Fig. 4a). The graph obtained from this analysis show a continuous heating of the nanocomposite up to 900 °C. In the entire sample, there was an initial weight loss of composite up to 120 °C. This attributes to loss of moisture on the nanocomposite surface. This was common for all nanocomposite studied in this work [9]. The thermal degradation of this composite can be seen in two major steps: first removal of surface moisture and secondly removal of cellulose and lignin; the

degradation of these two components is at 300 °C. Drastically, 50% of weight loss was seen after 300 °C till 900 °C. The thermal degradation of lignin occurs throughout the temperature [43]. The composite made from cellulose GO was also studied by TGA (Fig. 4b). The moisture loss was also evident in this analysis. But this composite was stable up to 350 °C; the % weight loss was minimum up to this temperature. The degradation of cellulose and hemicellulose was seen after this temperature. Fifty percent of the weight was lost from 350 to 450 °C, and then, there was a sudden drop in degradation which was slowly in progressing up to 650 °C. The inorganic residues were commonly degraded in this temperature range [21]. The composites prepared by coating activated carbon with surface functionalized graphene oxide with zirconium oxide were studied in TGA. The composite prepared had shown high thermal stability. There was up to 3.5% weight loss to the whole temperature degradation study. Only the moisture on the surface of the nanocomposite was removed at initial stage. The loss of volatile matter was found to be negligible in this composite (Fig. 4c). This result indicated a good surface coating, which had increased the thermal stability of the composite many folds. In up to 200 °C, no degradation was observed; after this temperature, a steady but minimum % weight loss was achieved till 900 °C. The high thermal stability of this composite made it more efficient for pollutant removal. The higher temperature tolerance is a bonus point for its utility in many industrial processes. The composite can be used high-temperature system. The activated carbon prepared from paralyzing chemically modified sawdust was shown in Fig. 4d. The temperature stability of the activated carbon was maintained up to 350 °C. Then, a sharp decrease in weight percentage was seen within 400 °C which gradually maintained up to 900 °C. The coating

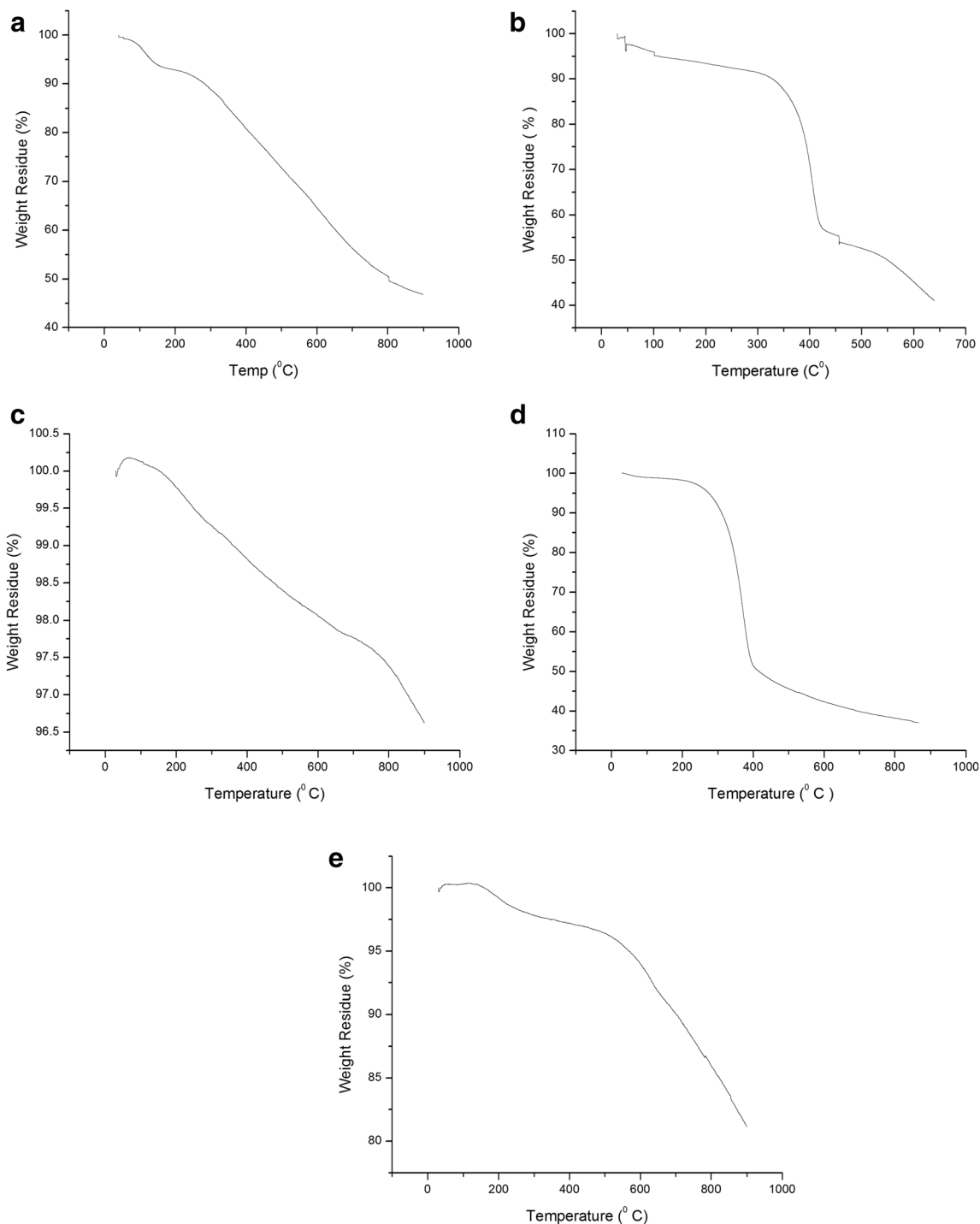


Fig. 4 Thermo-gravimetric analysis (TGA). **a** Activated carbon coated with graphene oxide. **b** Cellulose coated with graphene oxide. **c** Activated carbon coated with graphene oxide–zirconium oxide nanocomposite. **d** Thermally activated sawdust. **e** Activated carbon coated with zirconium oxide

of activated carbon with zirconium oxide had shown a steady weight loss (Fig. 4e). The metal coating had provided the composites with thermal stability than the normal activated carbon. This statement could be validated by comparing the graphs obtained from TGA analysis. The thermal stability study of the composites gives an

average estimation of the maximum bearable temperature by the adsorbent before it got degraded. Many industrial processes discharge high-temperature effluent water, and some adsorption process works better in higher temperature, so the thermal stability of the adsorbent plays an important role in the adsorption process.

3.1.5 BET analysis

BET analysis was done to estimate the surface area of the composite. The surface area is an important parameter for composite preparation. The higher the surface area, the higher would be the composite dispersion capability. All the samples were tested in BET analyzer (Autosorb-iQ-MP/XR, Quantachrome instruments, USA) by nitrogen adsorption method. The surface area (m^2/g) and the pore volume (cm^3/g) were obtained from this analysis. Table 1 shows the reports obtained from BET analysis. The composite prepared by coating GO with metals like lanthanum oxide, zirconium oxide, and cerium oxide was analyzed in BET analyzer, but the surface area obtained from these composites was less as compared with activated carbon-based composites. The composite prepared by coating cellulose with GO had also given lower surface area than the other activated carbon-based composites. The sawdust coated with GO and zirconium oxide had shown surface area of $96.979 \text{ m}^2/\text{g}$ and $138.45 \text{ m}^2/\text{g}$, respectively. The final composite prepared by coating the activated carbon with zirconium functionalized GO was found to be highest among all the composite studied. The surface area of this composite was found to be $314.842 \text{ m}^2/\text{g}$. The composite prepared by coating GO with cerium oxide had shown the lowest surface area among the entire composite, i.e., $9.890 \text{ m}^2/\text{g}$. The composite prepared from zirconium-coated GO was $25.342 \text{ m}^2/\text{g}$ and lanthanum-coated GO was found to be $16.446 \text{ m}^2/\text{g}$. The lower surface area of these composites can be due to agglomeration of metal oxide to the GO surface, causing the reduction in surface area. The analysis of activated carbon-based composites shows higher surface area than the graphene-based composites. The composites like activated carbon coated with GO and lanthanum oxide had provided more surface area due to its high surface area and high porosity. The metal coating had enhanced the surface area of the composite; the nanostructure of the metal oxide could be responsible for enhancing activated carbon surface. The coating of graphene oxide had lower surface area than the other activated carbon-based composites. The final composite studied was activated carbon coated with functionalized GO. The surface area obtained by analyzing this composite highest among

all the composites, i.e., $314.842 \text{ m}^2/\text{g}$. The higher surface area was obtained due to presence of activated carbon as the base material. All the activated carbon-based composites have high surface area; this can be due to presence micro- and mesopores on the surface of the activated carbon. The highly porous structure was able to accommodate the functionalized GO on to its surface. The mesopores were mainly responsible for this phenomenon. The functionalized GO was able to bind in the intricate channels of the activated carbon. The pore volume of this composite $0.101 \text{ cm}^3/\text{g}$ was higher than the others; the presence of higher number of pores was the determining factor for the composite formation. The presence of pores was directly proportional with the surface area as obtained by analyzing results from this study.

3.2 Removal efficiency of the nanocomposite

The removal of Cr^{+6} was optimized by analyzing the parameters like pH, adsorbent dose, and metal ion concentration.

The optimum pH obtained from studying these parameters was in acidic range, i.e., from pH 2 to 4 (Fig. 5a). The chromium species predominantly present in this range was HCrO_4^- . Mainly, three composites among the seven composites had responded efficiently in Cr^{+6} removals; among them, the activated carbon coated with surface functionalized graphene oxide was able to remove good amount of hexavalent chromium from the solution (14.67 mg/g). The composite prepared from coating activated carbon with zirconium oxide nanoparticle also showed a good removal capacity (8.41 mg/g). The other composites does not responded effectively in Cr^{+6} removal (0.09 mg/g for GO coated with CeO). The surface protonation always played an important role in Cr^{+6} removal; as the pH of the test solution increased, there may be the presence of more OH^- group on the solution, with a repulsion between the chromium species and the adsorption surface [40]. The deprotonating was found to be the main cause behind the lower removal efficiency of the composite at higher pH [34]. The effectiveness of these in acidic to neutral pH provided a solution for these composites in advanced waste water treatment technology. The inclination towards

Table 1 BET surface area of different composites

Sample name	Surface area (m^2/g)	Pore volume (cm^3/g)
GO-coated lanthanum oxide	16.446	0.006
GO-coated zirconium oxide	25.342	0.009
GO-coated cerium oxide	9.890	0.008
Sawdust coated with zirconium oxide	138.45	0.070
Cellulose coated with graphene oxide	22.550	0.008
Sawdust coated with GO	96.979	0.058
Sawdust coated with zirconium functionalized GO	314.842	0.101

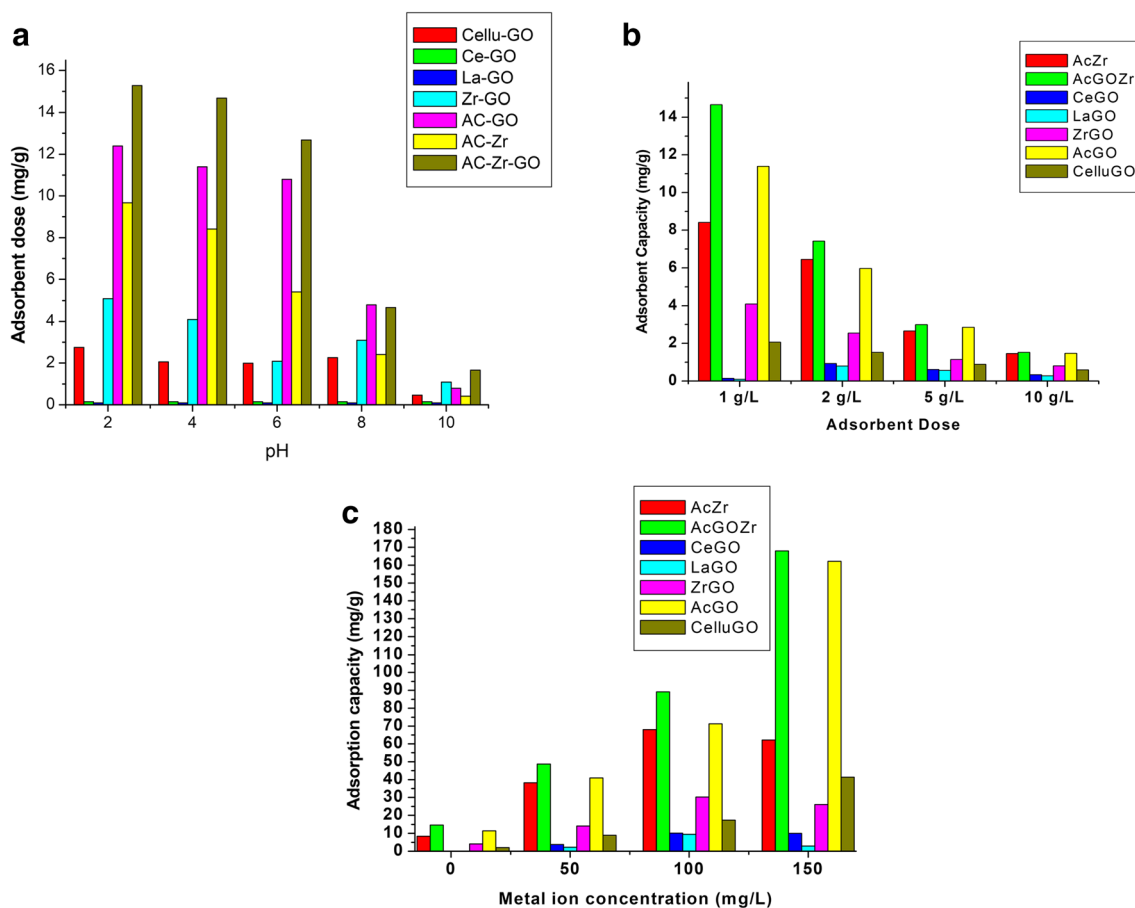


Fig. 5 a Adsorption capacity of various nanocomposites at various pH of the solution. b Adsorption capacity of nanocomposite at various doses for the removal of chromium solution. c Adsorption capacity of chromium at various initial concentrations of metal ion

acidic pH had shown regeneration capacity of the composite in alkaline solution.

The rest of the composite had lower affinity towards the Cr^{+6} removals and may be due to the lack of surface protonation and the presence of active surface functional group. From FTIR analysis, it was observed that the zirconium oxide–modified GO coating in activated carbon has provided many active functional groups in the composite. They were mainly hydroxyl, carbonyl, and hydronium ions; these active functional groups helped in binding the metal to the composite surface through weak chemical bonds. The surface active functional groups also played a vital role in attaching metal ion on the adsorbent surface. So surface protonation was not only the deterring factor for adsorption process, complexation, and chemical bonding; there could possibly be other factors responsible for the adsorption process.

The adsorbent dosage for Cr^{+6} removal was found to be an effective parameter in this study. The removal percentage was high with higher adsorbent dose which decreased with low adsorbent dosage. As the dosage of the composite increased, the adsorbent capacity decreased simultaneously (Fig. 5b) composites. The decrease in adsorbent capacity could be due to formation of intermolecular attraction between the nanocomposite particles as the concentration of composite

increased in a specific volume of metal ion solution [18]. The adsorbent dose for 1 mg/ml of metal ion solution was found to be high enough than the other selected adsorbent doses. In this study, the activated carbons coated with surface functionalized GO had higher adsorption capability than the other composites. The surface area of this composite was high as compared with other composites. The removal capability was second for activated carbon coated with GO and then activated carbon coated with zirconium oxide nanoparticles; the surface areas of this composites were found to be $314.842\text{ m}^2/\text{g}$, $96.979\text{ m}^2/\text{g}$, and $138.45\text{ m}^2/\text{g}$, respectively. These three composites had the highest surface area than the other composites, so they had the highest removal capacity than others. The lowest surface area observed among the composites was $9.890\text{ m}^2/\text{g}$, for GO coated with cerium oxide. The last parameter studied in this experiment was the capacity of the composite in removing high concentration of metal. The concentrations of Cr^{+6} studied were 10 mg/l, 50 mg/l, 100 mg/l, and 150 mg/l. The capacity of the composite to remove metal ion concentration was directly proportional to the concentration of metal ion (Fig. 5c). The composites synthesized in this study had highly porous structure. The higher the metal ion concentration, the higher would be the adherence of metal

into the surface of the composite. At high concentration, the availability of the metal ion was high and the chance of adherence of metal on the composite surface was also high. The pores present in the composite surface got higher chance for interaction between metal ion and the composite surface. So the surface active functional group got occupied with the metal ions more easily than the lower metal concentrations. Another factor was the effect of the metal oxide to reduce the Cr^{6+} , and then, chromium was adsorbed on the carbonaceous surface. It can be inferred that the removal efficiency of ZrO-graphene oxide-coated activated carbon was higher than the composite of graphene oxide-coated activated carbon (Fig. 5a–c). The availability of the functional groups also played an important role along with the number of pores present on the surface [4]. So the determining factor for this study was the pore volume, pore structure, catalytic activity of the metal ion, and active surface functional groups. The nanocomposites prepared by coating activated carbon with surface functionalized GO had the highest adsorption capacity. Due to its porous structure and presence of many oxygenated functional group onto its surface, the activated carbon coated with GO and lanthanum oxide comes to second and third places, respectively. The high concentration of metal ion had given a higher adsorbent capacity; above 160 mg/g of adsorbent capacity was obtained by the composite prepared from zirconium oxide GO-coated activated carbon and GO-coated activated carbon. The rest of the composites did not have this high adsorbent capacity. The high metal removing capacity for higher concentration of metal ion shows its potential usage in industrial application.

4 Conclusion

This study deals with synthesis of various nanocomposites namely activated carbon coated with surface functionalized GO with zirconium oxide, activated carbon coated with zirconium oxide, activated carbon coated with graphene oxide, graphene oxide coated with cerium oxide, graphene oxide coated with lanthanum oxide, graphene oxide coated with zirconium oxide, and cellulose coated with graphene oxide. Among all of the abovementioned composites, the activated carbon coated with surface functionalized GO with zirconium oxide, activated carbon coated with zirconium oxide, and activated carbon coated with graphene oxide had shown good characteristic features. These three composites had high amount of active surface functional group, surface area, and pore volume and pore structure. They had high thermal stability and crystalline structure. The efficiency of these composites was estimated by applying these composites in removing hexavalent chromium (Cr^{6+}). Parameters like pH, adsorbent dose, and metal ion concentration were studied. The pH study for Cr^{6+} removal was an important parameter, since the chromium species exist in different

forms in different pH. The acidic pH with 1 mg/ml adsorbent dose and up to 150 mg/l of hexavalent chromium could efficiently be removed by these three composites.

Funding The authors received financial assistance from the Science and Engineering Research Board, Department of Science and Technology (2018/EEQ/001309).

Compliance with ethical standards

Conflict of interest The authors declare that they have no conflict of interest.

References

1. Al-Zboon KK (2018) Phosphate removal by activated carbon–silica nanoparticles composite, kaolin, and olive cake. *Environ Dev Sustain* 20:2707–2724. <https://doi.org/10.1007/s10668-017-0012-z>
2. Chakraborty V, Das P (2020) Synthesis of nano-silica-coated biochar from thermal conversion of sawdust and its application for Cr removal: kinetic modelling using linear and nonlinear method and modelling using artificial neural network analysis. *Biomass Convers Biorefinery*. <https://doi.org/10.1007/s13399-020-01024-1>
3. Chakraborty V, Sengupta S, Chaudhuri P, Das P (2018) Assessment on removal efficiency of chromium by the isolated manglicolous fungi from Indian sundarban mangrove forest: removal and optimization using response surface methodology. *Environ Technol Innov* 10:335–344. <https://doi.org/10.1016/j.eti.2018.04.007>
4. Chakraborty V, Das P, Roy PK (2019) Carbonaceous materials synthesized from thermally treated waste materials and its application for the treatment of Strontium metal solution: Batch and optimization using Response Surface Methodology. *Environ Technol Innov* 15:100394. <https://doi.org/10.1016/j.eti.2019.100394>
5. Chakraborty V, Das P, Roy PK (2020) Synthesis and application of graphene oxide-coated biochar composite for treatment of strontium-containing solution. *Int J Environ Sci Technol*. <https://doi.org/10.1007/s13762-020-02930-7>
6. Chen W, Yu H, Liu Y, Chen P, Zhang M, Hai Y (2011) Individualization of cellulose nanofibers from wood using high-intensity ultrasonication combined with chemical pretreatments. *Carbohydr Polym* 83(4):1804–1811. <https://doi.org/10.1016/j.carbpol.2010.10.040>
7. Chen F, Yang Q, Zhong Y, An H, Zhao J, Xie T, Xu Q, Li X, Wang D, Zeng G (2016) Photo-reduction of bromate in drinking water by metallic Ag and reduced graphene oxide (RGO) jointly modified BiVO₄ under visible light irradiation. *Water Res* 101:555–563
8. Cho T-H, Shiosaki Y, Noguchi H (2006) Preparation and characterization of layered LiMn_{1/3}Ni_{1/3}Co_{1/3}O₂ as a cathode material by an oxalate co-precipitation method. *J Power Sources* 159(2): 1322–1327
9. Dai H, Huang H (2017) Synthesis, characterization and properties of pineapple peel cellulose-G-acrylic acid hydrogel loaded with kaolin and sepia ink. *Cellulose* 24:69–84. <https://doi.org/10.1007/s10570-016-1101-0>
10. Davis CH, Mathias LJ, Gilman JW, Schiraldi DA, Shields JR, Trulove P, Sutto TE, DeLong HC (2002) Effects of melt processing conditions on the quality of poly(ethylene terephthalate) montmorillonite clay nanocomposites. *J Polym Sci B Polym Phys* 40(23): 2661–2666
11. de Oliveira AAR, de Souza DA, Dias LLS, de Carvalho SM, Mansur HS, de Magalhães Pereira M (2013) Synthesis, characterization and cytocompatibility of spherical bioactive glass

- nanoparticles for potential hard tissue engineering applications. *Biomed Mater* 8(2):025011
12. El Rouby WMA, Farghali AA, Sadek MA, Khalil WF (2018) Fast removal of Sr(II) from water by graphene oxide and chitosan modified graphene oxide. *J Inorg Organomet Polym Mater* 28:2336–2349. <https://doi.org/10.1007/s10904-018-0885-9>
 13. Godinho MJ, Gonçalves RF, Santos LPS, Varela JA, Longo E, Leite ER (2007) Room temperature co-precipitation of nanocrystalline CeO₂ and Ce_{0.8}Gd_{0.2}O_{1.9-δ} powder. *Mater Lett* 61(8-9): 1904–1907
 14. Hussain F, Hojjati M, Okamoto M, Russell EG (2006) Review article: polymer-matrix nanocomposites, processing, manufacturing, and application: An Overview. *J Compos Mater* 40(17): 1511–1575. <https://doi.org/10.1177/0021998306067321>
 15. Introzzi L, Blomfeldt TOJ, Trabattionietal S (2012) Ultrasoundassisted pullulan/montmorillonite bionanocomposite coating with high oxygen barrier properties. *Langmuir* 28(30): 11206–11214. <https://doi.org/10.1021/la301781n>
 16. Jang J, Lee DS (2016) Enhanced adsorption of cesium on PVA-alginate encapsulated Prussian blue-graphene oxide hydrogel beads in a fixed-bed column system. *Bioresour Technol* 218:294–300. <https://doi.org/10.1016/j.biortech.2016.06.100>
 17. Johnson NR, Wang Y (2013) Controlled delivery of heparin-binding EGF-like growth factor yields fast and comprehensive wound healing. *J Control Release* 166:124–129. <https://doi.org/10.1016/j.jconrel.2012.11.004>
 18. Lingamdinne LP, Koduru JR, Chang YY, Kang SH, Yang JK (2019) Facile synthesis of flowered mesoporous graphene oxide-lanthanum fluoride nanocomposite for adsorptive removal of arsenic. *J Mol Liq* 279:32–42. <https://doi.org/10.1016/j.molliq.2019.01.103>
 19. Lu H, Gui Y, Zheng L, Liu X (2013) Morphological, crystalline, thermal and physicochemical properties of cellulose nanocrystals obtained from sweet potato residue. *Food Res Int* 50:121–128. <https://doi.org/10.1016/j.foodres.2012.10.013>
 20. Mahmoud, A.E.D., 2020. Nanomaterials: green synthesis for water applications, in: Handbook of nanomaterials and nanocomposites for energy and environmental applications. Springer International Publishing, Cham, pp. 1–21
 21. Mahmoud AED, Fawzy M, Hosny G, Obaid A (2020a) Equilibrium, kinetic, and diffusion models of chromium(VI) removal using *Phragmites australis* and *Ziziphus spina-christi* biomass. *Int J Environ Sci Technol*. <https://doi.org/10.1007/s13762-020-02968-7>
 22. Mahmoud AED, Franke M, Stelter M, Braeutigam P (2020b) Mechanochemical versus chemical routes for graphitic precursors and their performance in micropollutants removal in water. *Powder Technol* 366:629–640. <https://doi.org/10.1016/j.powtec.2020.02.073>
 23. Marcano DC, Kosynkin DV, Berlin JM, Sinitskii A, Sun Z, Slesarev A, Alemayehu LB, Lu W, Tour JM (2010) Improved synthesis of graphene oxide. *ACS Nano* 4(8):4806–4814. <https://doi.org/10.1021/nn1006368>
 24. Melikoğlu AY, Bilek SE, Cesur S (2019) Optimum alkaline treatment parameters for the extraction of cellulose and production of cellulose nanocrystals from apple pomace. *Carbohydr Polym* 215: 330–337. <https://doi.org/10.1016/j.carbpol.2019.03.103>
 25. Mingli C, Chunbao H, Mingli C, Chunbao H, Yikun L, Jianhua W (2016) Selective adsorption and efficient removal of phosphate from aqueous medium with graphene–lanthanum composite. *ACS Sustain Chem Eng* 4(3):1296–1302. <https://doi.org/10.1021/acssuschemeng.5b01324>
 26. Natália UY, Bergamasco R, Hamoudi S (2016) Magnetic MnFe₂O₄–graphene hybrid composite for efficient removal of glyphosate from water. *Chem Eng J* 295:391–402. <https://doi.org/10.1016/j.cej.2016.03.051>
 27. Nguyen TA, Nguyen H, Nguyen TV, Thai H, Shi X (2016) Effect of nanoparticles on the thermal and mechanical properties of epoxy coatings. *J Nanosci Nanotechnol* 16(9):9874–9881. <https://doi.org/10.1166/jnn.2016.12162>
 28. Nguyen-Tri P, Nguyen TA, Carriere P, Ngo Xuan C (2018) Nanocomposite coatings: preparation, characterization, properties, and applications. *Int J Corros* 2018:1–19. <https://doi.org/10.1155/2018/4749501>
 29. Qiu H, Liang C, Zhang X, Chen M, Zhao Y, Tao T, Xu Z, Liu G (2015) Fabrication of a biomass-based hydrous zirconium oxide nanocomposite for preferable phosphate removal and recovery. *ACS Appl Mater Interfaces* 7:20835–20844. <https://doi.org/10.1021/acsami.5b06098>
 30. Rani S, Aggarwal M, Kumar M, Sharma S, Kumar D (2016) Removal of methylene blue and rhodamine B from water by zirconium oxide/graphene. *Water Sci* 30:51–60. <https://doi.org/10.1016/j.wsj.2016.04.001>
 31. Rashidi Nodeh H, Sereshti H, Zamiri Afsharian E, Nouri N (2017) Enhanced removal of phosphate and nitrate ions from aqueous media using nanosized lanthanum hydrous doped on magnetic graphene nanocomposite. *J Environ Manag* 197:265–274. <https://doi.org/10.1016/j.jenvman.2017.04.004>
 32. Ravichandran K, Praseetha PK, Arun T, Gobalakrishnan S, 2018. Synthesis of Nanocomposites, Synthesis of Inorganic Nanomaterials. Elsevier Ltd. <https://doi.org/10.1016/b978-0-08-101975-7.00006-3>
 33. Reddy DHK, Sesaiah K, Reddy AVR, Rao MM, Wang MC (2010) Biosorption of Pb²⁺ from aqueous solutions by *Moringa oleifera* bark: equilibrium and kinetic studies. *J Hazard Mater* 174: 831–838. <https://doi.org/10.1016/j.jhazmat.2009.09.128>
 34. Rodrigues LA, Maschio LJ, Coppio LDSC, Thim GP, Silva MLCPD (2012) Adsorption of phosphate from aqueous solution by hydrous zirconium oxide. *Environ Technol* 33:1345–1351. <https://doi.org/10.1080/09593330.2011.632651>
 35. Saleem H, Haneef M, Abbasi HY (2018) Synthesis route of reduced graphene oxide via thermal reduction of chemically exfoliated graphene oxide. *Mater Chem Phys* 204:1–7. <https://doi.org/10.1016/j.matchemphys.2017.10.020>
 36. Santhi T, Manonmani S, Vasanthi VS, Chang YT (2016) A new alternative adsorbent for the removal of cationic dyes from aqueous solution. *Arab J Chem* 9:466–S474. <https://doi.org/10.1016/j.arabjc.2011.06.004>
 37. Shang M, Liu Y, Liu S, Zeng G, Tan X, Jiang L, Huang X, Ding Y, Guo Y, Wang S (2016) A novel graphene oxide coated biochar composite: synthesis, characterization and application for Cr(VI) removal. *RSC Adv* 6:85202–85212. <https://doi.org/10.1039/C6RA07151A>
 38. Shang Y, Wang Z, Xu X, Cheng C, Gao B, Yue Q, Liu S, Han C (2019) Enhanced fluoride uptake by bimetallic hydroxides anchored in cotton cellulose/graphene oxide composites. *J Hazard Mater* 376:91–101. <https://doi.org/10.1016/j.jhazmat.2019.05.039>
 39. Shi X, Nguyen TA, Suo Z, Liu Y, Avci R (2009) Effect of nanoparticles on the anticorrosion and mechanical properties of epoxy coating. *Surf Coat Technol* 204(3):237–245. <https://doi.org/10.1016/j.surfcoat.2009.06.048>
 40. Su J, Hao H, Lv X, Jin X, Yang Q (2020) Properties and mechanism of hexavalent chromium removal by FeS@ graphite carbon nitride nanocomposites. *Colloids Surf A Physicochem Eng Asp* 597: 124751. <https://doi.org/10.1016/j.colsurfa.2020.124751>
 41. Suganya Bharathi B, Stalin T (2019) Cerium oxide and peppermint oil loaded polyethylene oxide/graphene oxide electrospun nanofibrous mats as antibacterial wound dressings. *Mater Today Commun* 21: 100664. <https://doi.org/10.1016/j.mtcomm.2019.100664>
 42. Tuzen M, Sari A, Saleh TA (2018) Response surface optimization, kinetic and thermodynamic studies for effective removal of rhodamine B by magnetic AC/CeO₂ nanocomposite. *J Environ Manag* 206:170–177. <https://doi.org/10.1016/j.jenvman.2017.10.016>

43. Yang H, Yan R, Chen H, Lee DH, Zheng C (2007) Characteristics of hemicellulose, cellulose and lignin pyrolysis. *Fuel* 86:1781–1788. <https://doi.org/10.1016/j.fuel.2006.12.013>
44. Zhang X, Zhang L, Li A (2018) Eucalyptus sawdust derived biochar generated by combining the hydrothermal carbonization and low concentration KOH modification for hexavalent chromium removal. *J Environ Manag* 206:989–998. <https://doi.org/10.1016/j.jenvman.2017.11.079>
45. Zhang J, Zhang Z, Jiao Y, Yang H, Li Y, Zhang J, Gao P (2019) The graphene/lanthanum oxide nanocomposites as electrode materials of supercapacitors. *J. Power Sources* 419:99–105. <https://doi.org/10.1016/j.jpowsour.2019.02.059>
46. Wang H, Xie G, Fang M, Ying Z, Tong Y, Zeng Y (2017) Mechanical reinforcement of graphene/poly(vinyl chloride) composites prepared by combining the in-situ suspension polymerization and melt-mixing methods. *Compos B Eng* 113:278–284
47. Wang Z, Yu H, Xia J, Zhang F, Li F, Xia Y, Li Y (2012) Novel GO-blended PVDF ultrafiltration membranes. *Desalination* 299:50–54
48. Zhang CF, Zhong XC, Yu HY, Liu ZW, Zeng DC (2009) Effects of cobalt doping on the microstructure and magnetic properties of Mn–Zn ferrites prepared by the co-precipitation method. *Physica B: Condens Matter* 404(16):2327–2331

Publisher's Note Springer Nature remains neutral with regard to jurisdictional claims in published maps and institutional affiliations.